Hydrothermal synthesis of Mg/Al-layered double hydroxide modified water hyacinth hydrochar for remediation of wastewater containing mordant brown dye

Saadia M. Waly[1], Ahmad M. El-Wakil[1], Weam M. Abou El-Maaty[1], and Fathi S. Awad[1,2*]

[1]Chemistry Department, Faculty of Science, Mansoura University, Mansoura 35516, Egypt.
[2] Chemistry Department, Faculty of Science, New Mansoura University, New Mansoura 35712, Egypt.

Supporting Information

S1: Instruments

The WH, MgAl LDHs, MgAl@WH were characterized using a diversity of analytical techniques. Fourier transform infrared (FTIR) spectra were recorded using a Nicolet-Nexus 670 spectrometer equipped with a diamond ATR accessory. The measurement employed a resolution of 4 cm^{-1} and 32 scans. The crystal structure of the sample was analyzed using powder X-ray diffraction (XRD) on a PANalytical MPD X'Pert PRO diffractometer. The measurements employed 45 kV, 40 mA Ni-filtered Cu Kα1 radiation at room temperature. X-ray photoelectron spectra (XPS) were obtained on a Thermo-Fisher ESCALAB 250 spectrometer equipped with a micro-focused, monochromated Al Kα X-ray source operating at 15 kV and a double-focusing, full 180° spherical sector electron analyzer. Scanning electron microscopy (SEM): A Hitachi SU-70 field-SEM with an energy of 5.0 kV was used to take the SEM images. Transmission electron microscopy (TEM): A JEOL JEM1400 TEM was used to obtain the TEM images at 100 kV.

S2: Determination of pH$_{PZC}$

Solutions with pH between 2 and 12 were obtained by adding NaOH (0.1 M) or HCl (0.1 M) to Erlenmeyer flasks containing 50 mL of 0.01 M NaCl solution. Then, 0.15 g of the adsorbent was added to each flask; final pH measurements of the bottles were made after shaking for 48 h. The pH$_{PZC}$ of the sample is calculated from the point where pH$_{final}$ = pH$_{initial}$ crosses the curve between pH$_{final}$ and pH$_{initial}$.

Table S1: Remediation of various anionic dyes using MgAl LDH$_S$ and/or biochars prepared through different reported methods.

Adsorbent	Target dye	Qe (mg/g)	Ref.
Date palm derived biochar	Eriochrome black T	309.59	[1]
Date palm derived biochar	Methylene orange	163.12	[1]
MgAl-LDH	Methylene orange	197.62	[2]
MgAl-Charcoal activated	direct yellow	133.33	[3]
hydrochar from olive waste	Congo red	99.0	[4]
Mg/Al/ pine sawdust biochar	Methyl Orange (MO)	21.8	[5]
Mg/Al/ pine sawdust biochar	Sunset Yellow FCF (SYF	23.6	[5]
Biochar derived from Caulerpa scalpelliformis	Reactive Yellow 81	151.5	[6]
new biochar derived from pecan nutshell	Reactive red 141	130.0	[7]
Fe$_2$O$_3$–Biochar	Methyl Orange (MO)	46.6	[8]
functionalized magnetic bamboo biochar adsorbent	Methyl Orange (MO)	305.4	[9]
MgAl@WH	Mordant brown 15 dye	311.0	Present work

S3.

The Langmuir and Freundlich isotherm models are two extensively used mathematical models. The Langmuir model assumes a monolayer coverage and that all the adsorbent sorption sites are the same while the Freundlich isotherm model assumes that the coverage is multilayer and that all the adsorption sites are heterogenous. The Langmuir and Freundlich models are presented as Eq.(1) and Eq. [2], respectively, as follows:[10-11]

$$\ln q_e = lnK_f + \frac{1}{n} lnC_e \qquad (1)$$

$$\frac{C_e}{q_e} = \frac{1}{b\,Q_0} + \frac{C_e}{Q_0} \qquad (2)$$

Where q$_e$, C$_e$, b, and Q$_o$ are the equilibrium adsorption capacity, the equilibrium concentration of the metal ions, the Langmuir constant, and the Langmuir monolayer adsorption capacity, respectively. 1/n and K$_f$ are the adsorption intensity and the Freundlich constant, respectively.

Moreover, the essential feature of the Langmuir isotherm can be defined as RL parameter given by **Eq. (5)**.[12]

$$R_L = \frac{1}{1 + bc_0} \qquad (5)$$

The separation factor (R$_L$) can be used to indicate the shape of the adsorption behavior to be either irreversible (R$_L$ = 0), linear (R$_L$ = 1), unfavorable (R$_L$> 1), or favorable (0 < R$_L$ < 1).[13]

S4.

The PFO model usually predicts the behavior at the initial stage of the adsorption process, while PSO model predicts the behavior at all stages of the adsorption process[14].

Pseudo-first-order kinetic model:

$$\log\left(q_e - q_t\right) = \log q_e - \frac{K_1\, t}{2.303} \qquad (3)$$

Pseudo-second-order kinetic model:

$$\frac{t}{q_t} = \frac{1}{K_2 q_e^{\;2}} + \frac{t}{q_e} \qquad (4)$$

Where k_1 (min^{-1}) and k_2 (g mol^{-1} min^{-1}) are the rate constants. q_t and q_e are the adsorption uptake of heavy metal at time t (min) and at equilibrium. Where k_1 (min^{-1}) and k_2 (g mol^{-1} min^{-1}) are the rate constants. q_t and q_e are the adsorption uptake of heavy metal at time t (min) and at equilibrium.
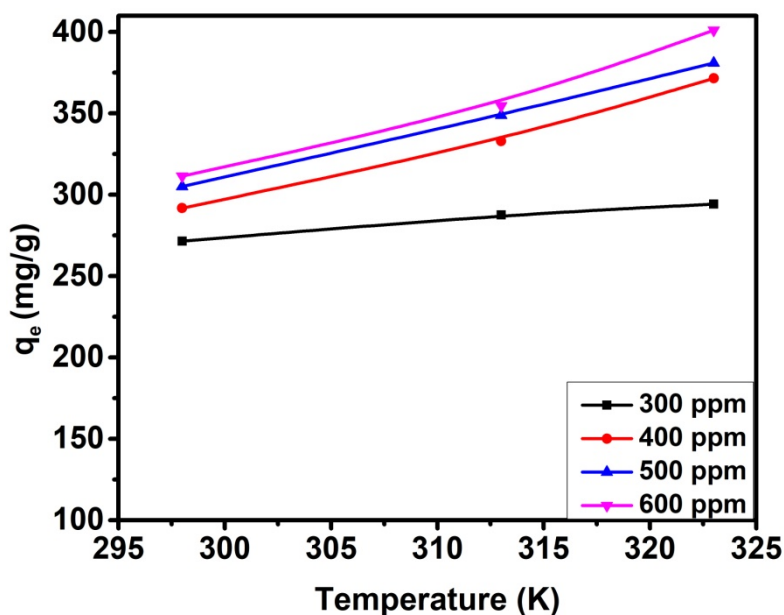

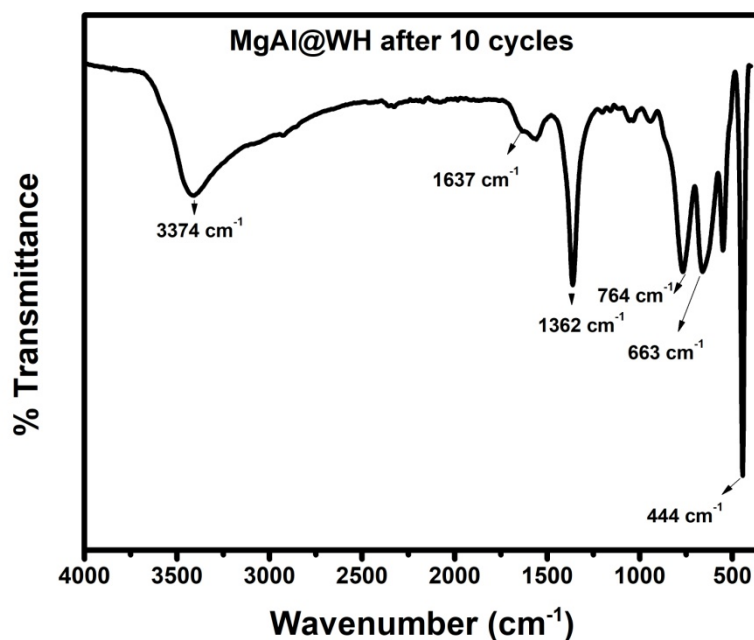Figure S1: Effect of temperature on mordant brown dye adsorption onto MgAl@WH.

Figure S2: FTIR spectra of MgAl@WH biochar after 10 cycles.

References

1. M. Zubair, N. D. Mu'azu, N. Jarrah, N. I. Blaisi, H. A. Aziz and M. A. Al-Harthi, *Water, Air, & Soil Pollution*, 2020, **231**, 1-19.
2. A. Zaghloul, R. Benhiti, A. A. Ichou, G. Carja, A. Soudani, M. Zerbet, F. Sinan and M. Chiban, *Materials Today: Proceedings*, 2021, **37**, 3793-3797.
3. N. Ahmad, F. S. Arsyad, I. Royani and A. Lesbani, *Results in Chemistry*, 2023, **5**, 100766.
4. M. Haris, M. W. Khan, J. Paz-Ferreiro, N. Mahmood and N. Eshtiaghi, *Chemical engineering journal advances*, 2022, **9**, 100233.
5. J. Kim, G.-H. Bak, D.-Y. Yoo, Y.-I. Lee, Y.-G. Lee and K. Chon, *Heliyon*, 2023, **9**.
6. M. L. Sundar, A. Aravindan, S. Sujatha, S. Mahendran, G. Kalyani, D. Z. Rahman, A. Vijayakumar and M. S. Kumar, *Biomass Conversion and Biorefinery*, 2020, 1-15.
7. M. A. Zazycki, M. Godinho, D. Perondi, E. L. Foletto, G. C. Collazzo and G. L. Dotto, *Journal of Cleaner Production*, 2018, **171**, 57-65.
8. N. Chaukura, E. C. Murimba and W. Gwenzi, *Applied Water Science*, 2017, **7**, 2175-2186.
9. H. Zhang, R. Li and Z. Zhang, *Environmental Pollution*, 2022, **293**, 118517.
10. F. S. Awad, K. M. AbouZied, W. M. Abou El-Maaty, A. M. El-Wakil and M. S. El-Shall, *Arabian Journal of Chemistry*, 2020, **13**, 2659-2670.
11. S. Pourbeyram, *Industrial & Engineering Chemistry Research*, 2016, **55**, 5608-5617.
12. F. A. Pavan, A. C. Mazzocato and Y. Gushikem, *Bioresource technology*, 2008, **99**, 3162-3165.

13. M. S. Alhumaimess, *Separation Science and Technology*, 2020, **55**, 1303-1316.
14. A. M. El-Wakil, S. M. Waly, W. M. Abou El-Maaty, M. M. Waly, M. Yılmaz and F. S. Awad, *ACS omega*, 2022, **7**, 6058-6069.